Reverberation mapping in the lamp-post geometry of the compact corona illuminating a black-hole accretion disc in AGN.

Michal Dovčiak[1], Erin Kara[2], Vladimír Karas[1], Barbara De Marco[3], Giorgio Matt[4], Giovanni Miniutti[5] and William Alston[2]

Abstract: The X-ray reverberation mapping of the inner parts of the accretion disc might be used to distinguish between different geometries of the corona. The basic properties of the reverberation mapping in the lamp-post geometry of the compact corona where the ionisation of the disc due to its illumination is taken into account are studied. The theoretical lag versus frequency and energy are shown for different model parameters such as the height of the corona, inclination of the observer, disc ionization profile and black hole spin. The influence of these parameters on the measured time lags are discussed. The results presented here will be tested by a future large X-ray observatory like Athena.

[1] Astronomical Institute, Academy of Sciences of the Czech Republic, Prague
[2] Institute of Astronomy, University of Cambridge, Cambridge
[3] Max-Planck-Institut für Extraterrestrische Physik, Garching
[4] Dipartimento di Matematica e Fisica, Università degli Studi "Roma Tre", Rome
[5] Centro de Astrobiología (CSIC-INTA), Departamento de Astrofísica, Madrid

The model components

Black hole: Schwarzschild or maximally rotating Kerr metric for central gravitating body with mass M and dimensionless spin parameter $a = 0$ or $a = 1$ is used.

Accretion disc: co-rotating, Keplerian, geometrically thin, optically thick, ionised disc extending from the innermost stable circular orbit (ISCO) up to the upper edge at $r_{\rm out} = 1000\,GM/c^2$.

Corona: hot point-like patch of plasma located on the rotation axis at the height h above the centre and emitting power-law radiation, $F_{\rm p}(E) \sim E^{-\Gamma}\,e^{-E/E_{\rm c}}$, with a sharp low energy cut-off at 0.1 keV and an exponential high energy cut-off at $E_{\rm c} = 300$ keV.

Observer: located at infinity, viewing the system with an inclination angle $\theta_{\rm o}$ with respect to the symmetry axis of the disc.

Figure 1: Sketch of the model

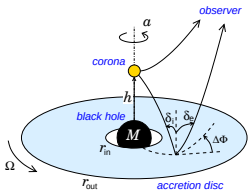

Approximations

Light rays: Full relativistic ray-tracing code in vacuum is used for photon paths from the corona to the disc and to the observer and from the disc to the observer.

Reflection: The REFLIONX, Ross & Fabian (2005), tables for constant density slab illuminated by the power-law incident radiation is used to compute the re-processing in the ionised accretion disc. The ionisation of the disc, ξ, is set by the amount of the incident primary flux (dependent on the luminosity of the primary source, height of the corona and mass of the black hole) and by the density of the accretion disc (different density radial profiles are used). We consider several limb brightening/darkening prescriptions for directionality of the re-processed emission.

Definitions

Transfer function – relative response of the disc to the illumination:

$$\psi_{\rm r}(E,t) = \frac{F_{\rm r}(E,t)}{F_{\rm p}(E)}, \qquad (1)$$

where $F_{\rm r}(E,t)$ is the time dependent observed reflected flux from the disc as a response to a flare that would be observed as $F_{\rm p}(E)\,\delta(t)$.

Fourier transform of the transfer function:

$$\hat{\psi}_{\rm r}(E,f) = A_{\rm r}(E,f)\,{\rm e}^{{\rm i}\varphi_{\rm r}(E,f)}, \qquad (2)$$

with the amplitude $A_{\rm r}(E,f)$ and phase $\varphi_{\rm r}(E,f)$.

Total phase – phase of the Fourier transform of the total flux, i.e. both the primary and reflected radiation are taken into account:

$$\varphi_{\rm tot}(E,f) = \operatorname{atan}\frac{A_{\rm r}(E,f)\,\sin\varphi_{\rm r}(E,f)}{1 + A_{\rm r}(E,f)\,\cos\varphi_{\rm r}(E,f)} \qquad (3)$$

Lag – computed from the total phase at energy bin E with respect to the total phase at some reference bin:

$$\tau(E,f) = \frac{\Delta\varphi_{\rm tot}(E,f)}{2\pi f}. \qquad (4)$$

The dependence of the lag between the flux in the soft excess energy band of $0.3 - 0.8$ keV and the flux in the reference energy band of $1 - 3$ keV on the system geometry (height of the corona, system inclination and spin of the black hole) and other parameters of the model (non-isotropy of the emission, photon index, energy band, ionisation of the disc) are shown in Fig. 2 and 3, respectively. The values of the parameters not explicitly stated in the figures are summarised in the following table:

parameter	value
inclination ($\theta_{\rm o}$)	30°
BH mass (M)	$10^8\,M_\odot$
BH spin (a)	1
height (h)	$3\,GM/c^2$
photon index (Γ)	2
intrinsic primary X-ray luminosity: $L_{\rm p} = 4\pi N_{\rm p}\int_{0.1}^{\infty} E^{-\Gamma+1}e^{-E/E_{\rm c}}$	$10^{-3}\,L_{\rm edd}$

The radial density profile of the disc was set to be:

$$n = 10^{14}\left(\frac{r}{GM/c^2}\right)^{-2}\ {\rm cm}^{-3}.$$

Lag spectrum

For small values of frequency, $f \lesssim 300\,\mu$Hz, the following holds true for the Fourier transform of the transfer function:

$$A_{\rm r}(E,f) \simeq A_{\rm r}(E)\,A_{\rm r}(f), \qquad (5)$$
$$\varphi_{\rm r}(E,f) \simeq \varphi_{\rm r}(f), \qquad (6)$$

with $A_{\rm r}(E) \simeq F_{\rm r}(E)/F_{\rm p}(E)$ and $A_{\rm r}(f) \lesssim 1$. It follows from the eq. (3) that the lag spectrum at frequencies $f_{\pm\pi/2}$ where

$$\varphi_{\rm r}(f_{\pm\pi/2}) = \pm\frac{\pi}{2} \qquad (7)$$

should be similar to the shape of the reflected photon flux, i.e.

$$\tau(E,f_{\pm\pi/2}) \simeq \frac{1}{2\pi f_{\pm\pi/2}}\operatorname{atan}\left[A_{\rm r}(f_{\pm\pi/2})\,\frac{F_{\rm r}(E)}{F_{\rm p}(E)}\right], \qquad (8)$$

where $F_{\rm r}(E)$ is the reflected flux integrated in time. Examples of such theoretical lag spectra are shown in Fig. 4 together with phases $\varphi_{\rm r}(f)$, $\Delta\varphi_{\rm tot}(E,f)$ and lag $\tau(E,f)$ where the lowest studied frequency, $f = 2.5\,\mu$Hz, and frequencies $f_{\pm\pi/2}$ fullfilling the condition (7) are depicted. Note that the shown absolute value of the time lag $|\tau(E,f_{\pm\pi/2})|$ was not taken with respect to any reference energy bin, and that the ratio $F_{\rm r}(E)/F_{\rm p}(E)$ at the bottom panels is shown to scale for comparison.

Conclusions

- The oscillations of the lag-frequency dependence, see Fig. 2, is due to wrapping of the Fourier phase of the disc response, $\varphi_{\rm r}(E,f)$, see eq. (3). This phase depends mainly on the geometry – height of the corona and observer inclination, and is almost independent on the spectral shape of the response.
- The magnitude and the exact shape of the lag-frequency plots depend on the spectral shape of the response, $A_{\rm r}(E,f)$, see eq. (3), and thus they depend on many details of the model – height, spin, ionisation, emission unisotropy, etc., see Fig. 3.
- The lag spectrum follows the spectral shape very well, the best agreement occurs at the lowest of the frequencies $f_{\pm\pi/2}$, see eqs. (7) – (8) and Fig. 4.

Acknowledgments

The research leading to these results has received funding from the European Union Seventh Framework Programme (FP7/2007 -2013) under grant agreement n°312789.

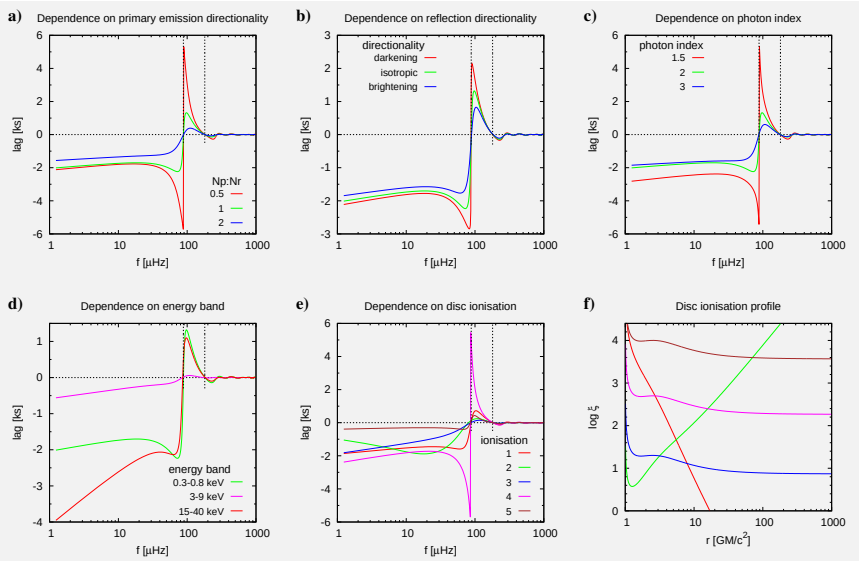

Figure 3: The dependence of lag on frequency for different (a) primary emission directionality with $N_{\rm p} : N_{\rm r}$ setting the ratio of the flux emitted towards the observer and towards the disc (per unit solid angle), (b) reflection directionality, (c) primary power-law photon index, (d) energy bands and (e) ionisation states of the accretion disc. (f) The disc ionisation profile used in panel (e) with corresponding colours – here, only the radial density profile of the disc was changed to get different radial ionisation profiles with all other parameters set as in previous graphs.

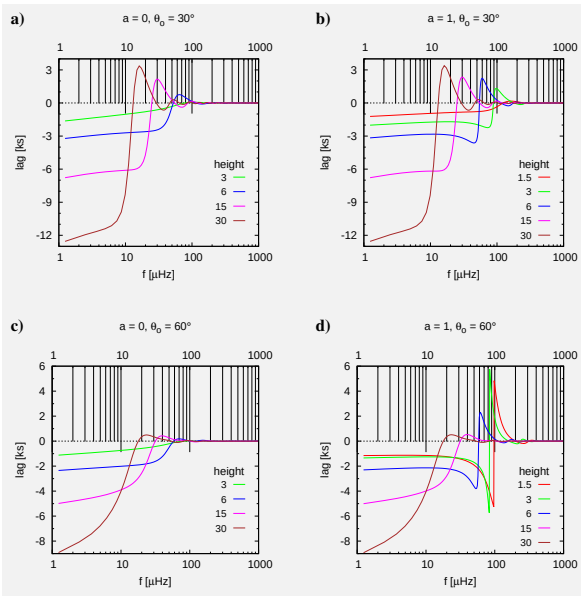

Figure 2: The dependence of lag on frequency for Schwarzshild BH ($a = 0$, left) and Kerr BH ($a = 1$, right) for observer's inclination of 30° (top) and 60° (bottom), and different height of the corona (units of GM/c^2, see colour scale in each panel).

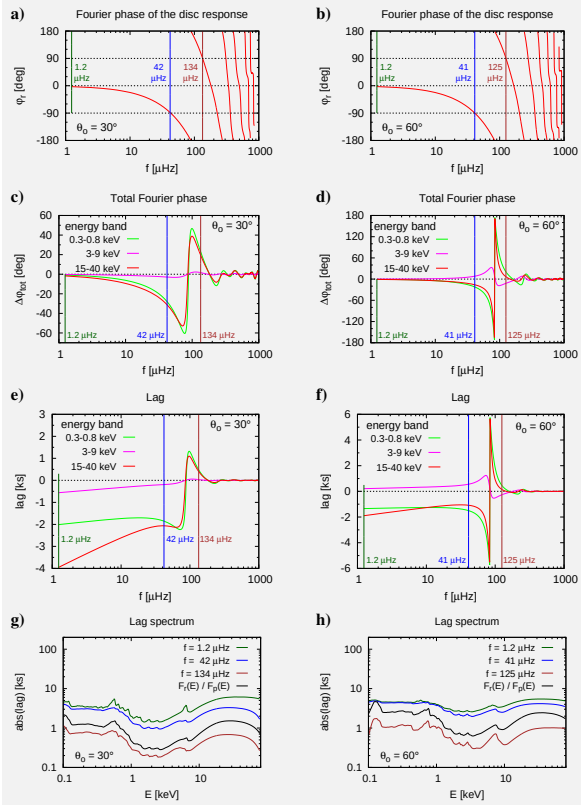

Figure 4: (a) – (b) The frequency dependence of Fourier phase of the transfer function, $\varphi_{\rm r}$, (c) – (d) difference of the total Fourier phase for different energy bands with respect to the reference energy band, $\Delta\varphi_{\rm tot}$, (e) – (f) corresponding lags, τ, (g) – (h) lag spectra at frequencies $2.5\,\mu$Hz and $f_{\pm\pi/2}$ and relative reflection spectra. The frequencies $2.5\,\mu$Hz and $f_{\pm\pi/2}$ are depicted in each panel.

e–mail: dovciak@asu.cas.cz